

## Measurement of inclusive jet cross sections in photoproduction at HERA

H1 Collaboration

I. Abt<sup>g</sup>, T. Ahmed<sup>c</sup>, V. Andreev<sup>x</sup>, B. Andrieu<sup>aa</sup>, R.-D. Appuhn<sup>k</sup>, M. Arpagaus<sup>ah</sup>, A. Babaev<sup>y</sup>, H. Bärwolff<sup>ag</sup>, J. Bán<sup>q</sup>, P. Baranov<sup>x</sup>, E. Barrelet<sup>ab</sup>, W. Bartel<sup>k</sup>, U. Bassler<sup>ab</sup>, H.P. Beck<sup>ai</sup>, H.-J. Behrend<sup>k</sup>, A. Belousov<sup>x</sup>, Ch. Berger<sup>a</sup>, H. Bergstein<sup>a</sup>, G. Bernardi<sup>ab</sup>, R. Bernet<sup>ah</sup>, G. Bertrand-Coremans<sup>d</sup>, M. Besançon<sup>i</sup>, P. Biddulph<sup>v</sup>, E. Binder<sup>k</sup>, A. Bischoff<sup>ag</sup>, J.C. Bizot<sup>z</sup>, V. Blobel<sup>m</sup>, K. Borras<sup>h</sup>, P.C. Bosetti<sup>b</sup>, V. Boudry<sup>aa</sup>, C. Bourdarios<sup>z</sup>, F. Brasse<sup>k</sup>, U. Braun<sup>b</sup>, W. Braunschweig<sup>a</sup>, V. Brisson<sup>z</sup>, D. Bruncko<sup>q</sup>, L. Büngener<sup>m</sup>, J. Bürger<sup>k</sup>, F.W. Büsser<sup>m</sup>, A. Buniatian<sup>ki</sup>, S. Burke<sup>s</sup>, G. Buschhorn<sup>y</sup>, A.J. Campbell<sup>j</sup>, T. Carli<sup>v</sup>, F. Charles<sup>ab</sup>, D. Clarke<sup>e</sup>, A.B. Clegg<sup>r</sup>, M. Colombo<sup>h</sup>, J.A. Coughlan<sup>e</sup>, A. Courau<sup>z</sup>, Ch. Coutures<sup>i</sup>, G. Cozzika<sup>i</sup>, L. Criegee<sup>k</sup>, J. Cvach<sup>aa</sup>, S. Dagoret<sup>ab</sup>, J.B. Dainton<sup>s</sup>, M. Danilov<sup>w</sup>, A.W.E. Dann<sup>v</sup>, W.D. Dau<sup>p</sup>, M. David<sup>i</sup>, E. Deffur<sup>k</sup>, B. Delcourt<sup>z</sup>, L. Del Buono<sup>ab</sup>, M. Devel<sup>z</sup>, A. De Roeck<sup>k</sup>, P. Dingus<sup>aa</sup>, C. Dollfus<sup>ai</sup>, J.D. Dowell<sup>c</sup>, H.B. Dreis<sup>b</sup>, A. Drescher<sup>h</sup>, J. Duboc<sup>ab</sup>, D. Düllmann<sup>m</sup>, O. Dünker<sup>m</sup>, H. Duhm<sup>l</sup>, R. Ebbinghaus<sup>h</sup>, M. Eberle<sup>l</sup>, J. Ebert<sup>af</sup>, T.R. Ebert<sup>s</sup>, G. Eckerlin<sup>k</sup>, V. Efremenko<sup>w</sup>, S. Egli<sup>ai</sup>, S. Eichenberger<sup>ai</sup>, R. Eichler<sup>ah</sup>, F. Eisele<sup>n</sup>, E. Eisenhandler<sup>i</sup>, N.N. Ellis<sup>c</sup>, R.J. Ellison<sup>v</sup>, E. Elsen<sup>k</sup>, M. Erdmann<sup>n</sup>, E. Evrard<sup>d</sup>, L. Favart<sup>d</sup>, A. Fedotov<sup>w</sup>, D. Feecken<sup>m</sup>, R. Felst<sup>k</sup>, J. Feltesse<sup>i</sup>, I.F. Fensome<sup>c</sup>, J. Ferencei<sup>k</sup>, F. Ferrarotto<sup>ae</sup>, K. Flamm<sup>k</sup>, W. Flauger<sup>k,2</sup>, M. Fleischer<sup>k</sup>, G. Flüge<sup>b</sup>, A. Fomenko<sup>x</sup>, B. Fominykh<sup>w</sup>, M. Forbush<sup>g</sup>, J. Formánek<sup>ad</sup>, J.M. Foster<sup>v</sup>, G. Franke<sup>k</sup>, E. Fretwurst<sup>l</sup>, P. Fuhrmann<sup>a</sup>, E. Gabathuler<sup>s</sup>, K. Gamerding<sup>y</sup>, J. Garvey<sup>c</sup>, J. Gayler<sup>k</sup>, A. Gellrich<sup>m</sup>, M. Gennis<sup>k</sup>, H. Genzel<sup>a</sup>, R. Gerhards<sup>k</sup>, L. Godfrey<sup>g</sup>, U. Goerlach<sup>k</sup>, L. Goerlich<sup>f</sup>, M. Goldberg<sup>ab</sup>, A.M. Goodall<sup>s</sup>, I. Gorelov<sup>w</sup>, P. Goritchev<sup>w</sup>, C. Grab<sup>ah</sup>, H. Grässler<sup>b</sup>, R. Grässler<sup>b</sup>, T. Greenshaw<sup>s</sup>, H. Greif<sup>y</sup>, G. Grindhammer<sup>y</sup>, C. Gruber<sup>p</sup>, J. Haack<sup>ag</sup>, D. Haidt<sup>k</sup>, L. Hajduk<sup>f</sup>, O. Hamon<sup>ab</sup>, D. Handschuh<sup>k</sup>, E.M. Hanlon<sup>r</sup>, M. Hapke<sup>k</sup>, J. Harjes<sup>k</sup>, R. Haydar<sup>z</sup>, W.J. Haynes<sup>e</sup>, J. Heatherington<sup>i</sup>, V. Hedberg<sup>u</sup>, G. Heinzelmann<sup>m</sup>, R.C.W. Henderson<sup>r</sup>, H. Henschel<sup>ag</sup>, R. Herma<sup>a</sup>, I. Herynek<sup>ac</sup>, W. Hildesheim<sup>ab</sup>, P. Hill<sup>k</sup>, C.D. Hilton<sup>v</sup>, J. Hladký<sup>ac</sup>, K.C. Hoeger<sup>v</sup>, Ph. Huet<sup>d</sup>, H. Hufnagel<sup>n</sup>, N. Huot<sup>ab</sup>, M. Ibbotson<sup>v</sup>, H. Itterbeck<sup>a</sup>, M.-A. Jabiol<sup>i</sup>, A. Jacholkowska<sup>z</sup>, C. Jacobsson<sup>u</sup>, M. Jaffre<sup>z</sup>, T. Jansen<sup>k</sup>, L. Jönsson<sup>u</sup>, K. Johannsen<sup>m</sup>, D.P. Johnson<sup>d</sup>, L. Johnson<sup>r</sup>, H. Jung<sup>b</sup>, P.I.P. Kalmus<sup>i</sup>, S. Kasarian<sup>k</sup>, R. Kaschowitz<sup>b</sup>, P. Kassermann<sup>l</sup>, U. Kathage<sup>p</sup>, H. H.Kaufmann<sup>ag</sup>, I.R. Kenyon<sup>c</sup>, S. Kermiche<sup>z</sup>, C. Keuker<sup>a</sup>, C. Kiesling<sup>y</sup>, M. Klein<sup>ag</sup>, C. Kleinwort<sup>m</sup>, G. Knies<sup>k</sup>, W. Ko<sup>g</sup>, T. Köhler<sup>a</sup>, H. Kolanoski<sup>h</sup>, F. Kole<sup>g</sup>, S.D. Kolya<sup>v</sup>, V. Korbel<sup>k</sup>, M. Korn<sup>h</sup>, P. Kostka<sup>ag</sup>, S.K. Kotelnikov<sup>x</sup>, M.W. Krasny<sup>f,ab</sup>, H. Krehbiel<sup>k</sup>, D. Krücker<sup>b</sup>, U. Krüger<sup>k</sup>, J.P. Kubenka<sup>y</sup>, H. Küster<sup>b</sup>, M. Kuhlen<sup>y</sup>, T. Kurča<sup>q</sup>, J. Kurzhöfer<sup>h</sup>, B. Kuznik<sup>af</sup>, F. Lamarche<sup>aa</sup>, R. Lander<sup>g</sup>, M.P.J. Landon<sup>i</sup>, W. Lange<sup>ag</sup>, R. Langkau<sup>l</sup>, P. Lanus<sup>y</sup>, J.F. Laporte<sup>i</sup>, A. Lebedev<sup>x</sup>, A. Leuschner<sup>k</sup>, C. Leverenz<sup>k</sup>, S. Levonian<sup>k,x</sup>, D. Lewin<sup>k</sup>, Ch. Ley<sup>b</sup>, A. Lindner<sup>h</sup>, G. Lindström<sup>l</sup>, F. Linsel<sup>k</sup>, J. Lipinski<sup>m</sup>, P. Loch<sup>k</sup>, H. Lohmander<sup>u</sup>, G.C. Lopez<sup>t</sup>, D. Lüers<sup>y,2</sup>, N. Magnussen<sup>af</sup>, E. Malinovski<sup>x</sup>, S. Mani<sup>g</sup>, P. Marage<sup>d</sup>, J. Marks<sup>j</sup>, R. Marshall<sup>v</sup>, J. Martens<sup>af</sup>, R. Martin<sup>s</sup>, H.-U. Martyn<sup>a</sup>, J. Martyniak<sup>f</sup>, S. Masson<sup>b</sup>, A. Mavroidis<sup>t</sup>, S.J. Maxfield<sup>s</sup>, S.J. McMahon<sup>s</sup>, A. Mehta<sup>v</sup>, K. Meier<sup>o</sup>, D. Mercer<sup>v</sup>, T. Merz<sup>k</sup>, C.A. Meyer<sup>ai</sup>, H. Meyer<sup>af</sup>, J. Meyer<sup>k</sup>, S. Mikocki<sup>f,z</sup>, V. Milone<sup>ac</sup>, E. Monnier<sup>ab</sup>, F. Moreau<sup>aa</sup>, J. Moreels<sup>d</sup>,

J.V. Morris<sup>e</sup>, K. Müller<sup>ai</sup>, P. Murin<sup>q</sup>, S.A. Murray<sup>v</sup>, V. Nagovizin<sup>w</sup>, B. Naroska<sup>m</sup>,  
 Th. Naumann<sup>ag</sup>, D. Newton<sup>r</sup>, D. Neyret<sup>ab</sup>, H.K. Nguyen<sup>ab</sup>, F. Niebergall<sup>m</sup>, R. Nisius<sup>a</sup>,  
 G. Nowak<sup>f</sup>, G.W. Noyes<sup>c</sup>, M. Nyberg<sup>u</sup>, H. Oberlack<sup>y</sup>, U. Obrock<sup>h</sup>, J.E. Olsson<sup>k</sup>, S. Orenstein<sup>aa</sup>,  
 F. Ould-Saada<sup>m</sup>, C. Pascaud<sup>z</sup>, G.D. Patel<sup>s</sup>, E. Peppel<sup>k</sup>, S. Peters<sup>y</sup>, H.T. Phillips<sup>c</sup>, J.P. Phillips<sup>y</sup>,  
 Ch. Pichler<sup>l</sup>, W. Pilgram<sup>b</sup>, D. Pitzl<sup>ah</sup>, S. Prell<sup>k</sup>, R. Prosi<sup>k</sup>, G. Rädcl<sup>k</sup>, F. Raupach<sup>a</sup>,  
 K. Rauschnabel<sup>h</sup>, P. Reimer<sup>ac</sup>, P. Ribarics<sup>y</sup>, V. Riech<sup>l</sup>, J. Riedlberger<sup>ah</sup>, S. Riess<sup>m</sup>, M. Rietz<sup>b</sup>,  
 S.M. Robertson<sup>c</sup>, P. Robmann<sup>ai</sup>, R. Roosen<sup>d</sup>, A. Rostovtsev<sup>w</sup>, C. Royon<sup>i</sup>, M. Rudowicz<sup>y</sup>,  
 M. Ruffer<sup>l</sup>, S. Rusakov<sup>x</sup>, K. Rybicki<sup>f</sup>, N. Sahlmann<sup>b</sup>, E. Sanchez<sup>y</sup>, D.P.C. Sankey<sup>e</sup>,  
 M. Savitsky<sup>k</sup>, P. Schacht<sup>y</sup>, P. Schleper<sup>n</sup>, W. von Schlippe<sup>l</sup>, C. Schmidt<sup>k</sup>, D. Schmidt<sup>af</sup>,  
 W. Schmitz<sup>b</sup>, V. Schröder<sup>k</sup>, M. Schulz<sup>k</sup>, A. Schwind<sup>ag</sup>, W. Scobel<sup>l</sup>, U. Seehausen<sup>m</sup>, R. Sell<sup>k</sup>,  
 A. Semenov<sup>w</sup>, V. Shekelyan<sup>w</sup>, I. Sheviakov<sup>x</sup>, H. Shooshtari<sup>y</sup>, L.N. Shtarkov<sup>x</sup>, G. Siegmö<sup>p</sup>,  
 U. Siewert<sup>p</sup>, Y. Sirois<sup>aa</sup>, I.O. Skillicorn<sup>j</sup>, P. Smirnov<sup>x</sup>, J.R. Smith<sup>g</sup>, L. Smolik<sup>k</sup>, Y. Soloviev<sup>x</sup>,  
 H. Spitzer<sup>m</sup>, P. Staroba<sup>ac</sup>, M. Steenbock<sup>m</sup>, P. Steffen<sup>k</sup>, R. Steinberg<sup>b</sup>, B. Stella<sup>ac</sup>, K. Stephens<sup>y</sup>,  
 J. Stier<sup>k</sup>, U. Stösslein<sup>ag</sup>, J. Strachota<sup>k</sup>, U. Straumann<sup>ai</sup>, W. Struczinski<sup>b</sup>, J.P. Sutton<sup>c</sup>,  
 R.E. Taylor<sup>aj,z</sup>, V. Tchernyshov<sup>w</sup>, C. Thiebaut<sup>aa</sup>, G. Thompson<sup>l</sup>, I. Tichomirov<sup>w</sup>, P. Truöl<sup>ai</sup>,  
 J. Turnau<sup>f</sup>, J. Tutas<sup>n</sup>, L. Urban<sup>y</sup>, A. Usik<sup>x</sup>, S. Valkar<sup>ad</sup>, A. Valkarova<sup>ad</sup>, C. Vallée<sup>ab</sup>,  
 P. Van Esch<sup>d</sup>, A. Vartapetian<sup>k,l</sup>, Y. Vazdik<sup>x</sup>, M. Vecko<sup>ac</sup>, P. Verrecchia<sup>i</sup>, R. Vick<sup>m</sup>, G. Villet<sup>i</sup>,  
 E. Vogel<sup>a</sup>, K. Wacker<sup>h</sup>, I.W. Walker<sup>r</sup>, A. Walther<sup>h</sup>, G. Weber<sup>m</sup>, D. Wegener<sup>h</sup>, A. Wegner<sup>k</sup>,  
 H. P.Wellsch<sup>y</sup>, S. Willard<sup>g</sup>, M. Winde<sup>ag</sup>, G.-G. Winter<sup>k</sup>, Th. Wolff<sup>ah</sup>, L.A. Womersley<sup>s</sup>,  
 A.E. Wright<sup>v</sup>, N. Wulff<sup>k</sup>, T.P. Yiou<sup>ab</sup>, J. Žáček<sup>ad</sup>, P. Závada<sup>ac</sup>, C. Zeitnitz<sup>l</sup>, H. Ziaepour<sup>z</sup>,  
 M. Zimmer<sup>k</sup>, W. Zimmermann<sup>k</sup> and F. Zomer<sup>z</sup>

<sup>a</sup> I. Physikalisches Institut der RWTH, Aachen, Germany <sup>3</sup>

<sup>b</sup> III. Physikalisches Institut der RWTH, Aachen, Germany <sup>3</sup>

<sup>c</sup> School of Physics and Space Research, University of Birmingham, Birmingham, UK <sup>4</sup>

<sup>d</sup> Inter-University Institute for High Energies ULB-VUB, Brussels, Belgium <sup>5</sup>

<sup>e</sup> Rutherford Appleton Laboratory, Chilton, Didcot, UK <sup>4</sup>

<sup>f</sup> Institute for Nuclear Physics, Cracow, Poland <sup>6</sup>

<sup>g</sup> Physics Department and IIRPA, University of California, Davis, CA, USA <sup>7</sup>

<sup>h</sup> Institut für Physik, Universität Dortmund, Dortmund, Germany <sup>3</sup>

<sup>i</sup> DAPNIA, Centre d'Etudes de Saclay, Gif-sur-Yvette, France

<sup>j</sup> Department of Physics and Astronomy, University of Glasgow, Glasgow, UK <sup>4</sup>

<sup>k</sup> DESY, Hamburg, Germany <sup>3</sup>

<sup>l</sup> I. Institut für Experimentalphysik, Universität Hamburg, Hamburg, Germany <sup>3</sup>

<sup>m</sup> II. Institut für Experimentalphysik, Universität Hamburg, Hamburg, Germany <sup>3</sup>

<sup>n</sup> Physikalisches Institut, Universität Heidelberg, Heidelberg, Germany <sup>3</sup>

<sup>o</sup> Institut für Hochenergiephysik, Universität Heidelberg, Heidelberg, Germany <sup>3</sup>

<sup>p</sup> Institut für Reine und Angewandte Kernphysik, Universität Kiel, Kiel, Germany <sup>3</sup>

<sup>q</sup> Institute of Experimental Physics, Slovak Academy of Sciences, Košice, Slovak Republik

<sup>r</sup> School of Physics and Materials, University of Lancaster, Lancaster, UK <sup>4</sup>

<sup>s</sup> Department of Physics, University of Liverpool, Liverpool, UK <sup>4</sup>

<sup>t</sup> Queen Mary and Westfield College, London, UK <sup>4</sup>

<sup>u</sup> Physics Department, University of Lund, Lund, Sweden <sup>8</sup>

<sup>v</sup> Physics Department, University of Manchester, Manchester, UK <sup>4</sup>

<sup>w</sup> Institute for Theoretical and Experimental Physics, Moscow, Russia

<sup>x</sup> Lebedev Physical Institute, Moscow, Russia

<sup>y</sup> Max-Planck-Institut für Physik, München, Germany <sup>3</sup>

<sup>z</sup> LAL, Université de Paris-Sud, IN2P3-CNRS, Orsay, France

<sup>aa</sup> LPNHE, Ecole Polytechnique, IN2P3-CNRS, Palaiseau, France

<sup>ab</sup> LPNHE, Universités Paris VI and VII, IN2P3-CNRS, Paris, France

<sup>ac</sup> Institute of Physics, Czech Academy of Sciences, Praha, Czech Republik

<sup>ad</sup> Nuclear Center, Charles University, Praha, Czech Republik

<sup>ae</sup> INFN Roma and Dipartimento di Fisica, Universita "La Sapienza", Roma, Italy

<sup>af</sup> Fachbereich Physik, Bergische Universität Gesamthochschule Wuppertal, Wuppertal, Germany <sup>3</sup>

<sup>ag</sup> DESY, Institut für Hochenergiephysik, Zeuthen, Germany<sup>3</sup>

<sup>ah</sup> Institut für Mittelenergiephysik, ETH, Zürich, Switzerland<sup>9</sup>

<sup>ai</sup> Physik-Institut der Universität Zürich, Zürich, Switzerland<sup>9</sup>

<sup>aj</sup> Stanford Linear Accelerator Center, Stanford, CA, USA

Received 22 July 1993

Editor: K. Winter

The inclusive jet cross section in photoproduction has been measured as a function of transverse energy and pseudorapidity using the H1 detector at the HERA electron–proton collider. The results are compared with leading order QCD calculations.

High transverse energy,  $E_t$ , jets from photoproduction events have recently been reported by the H1 and ZEUS experiments at the electron–proton collider HERA [1,2]. Here quasi-real photons are produced by beam electrons scattering through small angles. In the framework of QCD these photons are probed by both the quarks and the gluons of the beam protons. Two types of mechanism contribute to the production of jets: the partons from the proton can interact with the photon either electrodynamically (directly) or with the quark and gluon content of the photon. The latter, so-called resolved mechanism, is described in terms of a photon structure function and is expected [3] to dominate in the kinematic region studied.

So far information on the photon structure function has been obtained in deep-inelastic  $e\gamma$  scattering experiments at  $e^+e^-$  colliders. The theoretical parametrizations of the photon structure functions derived from these measurements constrain mainly the

quark and antiquark contributions but allow for large differences in the gluon content. Recent experimental analyses of jet production in  $\gamma\gamma$  collisions [4] show sensitivity to the gluon content of the photon but are limited by theoretical uncertainties in the calculation of the jet cross section at relatively low  $E_t$ . The measurements of high- $E_t$  jet production at HERA will further constrain the gluon content of the photon and will also test a variety of QCD predictions.

This letter presents the first measurement of an  $ep$  inclusive jet cross section in the interactions of quasi-real photons with protons at HERA. The analysis is based on data collected with the H1 detector during 1992 which correspond to an integrated luminosity of  $25 \text{ nb}^{-1}$ .

The HERA  $ep$  storage ring was operated with 9 colliding bunches of  $e^-$  and  $p$  each, with energies of 26.7 GeV and 820 GeV respectively. The H1 detector is described elsewhere [5,6]. Here we describe briefly the components of the detector relevant to this analysis.

The tracking system consists of a central drift chamber supplemented by a forward track detector. It was used for the reconstruction of the charged particle tracks and the interaction vertex. The central chamber is interleaved with an inner and an outer double layer of cylindrical multiwire proportional chambers (MWPC) which were used in the trigger to select events with charged tracks pointing to the interaction region.

The tracking system is surrounded by a fine grained liquid argon (LAr) calorimeter [7] consisting of an electromagnetic section with lead absorbers and a hadronic section with steel absorbers.

<sup>1</sup> Visitor from Yerevan Phys. Inst., Armenia.

<sup>2</sup> Deceased.

<sup>3</sup> Supported by the Bundesministerium für Forschung und Technologie, FRG, under contract numbers 6AC17P, 6AC47P, 6DO57I, 6HH17P, 6HH27I, 6HD17I, 6HD27I, 6KI17P, 6MP17I, and 6WT87P.

<sup>4</sup> Supported by the UK Science and Engineering Research Council.

<sup>5</sup> Supported by IISN-IKW, NATO CRG-890478.

<sup>6</sup> Supported by the Polish State Committee for Scientific Research, grant No. 204209101.

<sup>7</sup> Supported in part by USDOE grant DE F603 91ER40674.

<sup>8</sup> Supported by the Swedish Natural Science Research Council.

<sup>9</sup> Supported by the Swiss National Science Foundation.

The energy resolutions achieved in test beams were  $\sigma/E \approx 12\%/\sqrt{E}$  for electrons and  $\approx 50\%/\sqrt{E}$  for pions [6–8]. The LAr calorimeter covers the complete azimuth and the range from  $-1.5$  to  $3.3$  in pseudorapidity  $\eta = -\ln(\tan(\theta/2))$ . Here  $\theta$  is the polar angle with respect to the proton beam direction ( $z$  axis). The backward region ( $-3.3 < \eta < -1.5$ ) is covered by a lead-scintillator electromagnetic calorimeter (BEMC). For the measurement of the hadronic energy flow we use the cells of the LAr calorimeter and of the BEMC. The reconstruction of calorimetric energies is described in more detail in [6,8]. The calorimeters and the tracking system are placed inside a superconducting solenoid which, together with the surrounding octagonal iron yoke, maintains a uniform magnetic field of  $1.2$  T along  $z$  in the tracking region. An electron detector, which is a part of the luminosity measuring system, “tags” photoproduction processes by detecting electrons scattered at small angles  $\theta' < 5$  mrad ( $\theta' = \pi - \theta$ ). The detector is a TlCl/TlBr crystal Cerenkov calorimeter with an energy resolution of  $10\%/\sqrt{E}$ .

A coincidence of the small angle electron detector signal ( $E' > 4$  GeV) with at least one track pointing to the vertex region was used to trigger on events from interactions of protons with quasi-real photons. The track condition is derived from the cylindrical MWPC and requires  $p_t \gtrsim 150\text{MeV}/c$ . More details of the trigger conditions can be found in [9]. The events retained by this trigger condition were processed through the H1 event reconstruction program. The events were accepted only if the reconstructed vertex was found to be within the interaction region ( $|z| < 44$  cm, with the nominal interaction point at  $z = 0$ ). The loss due to events outside this region was determined to be  $(12 \pm 2)\%$  using a track independent trigger. Events containing cosmic ray showers and beam halo muons were rejected using pattern recognition in the central tracking system and in the LAr calorimeter. For the remaining events we required the fractional energy of the photon measured in the small angle electron detector to have  $0.25 < y < 0.7$ , where

$$y = 1 - E'/E$$

and  $E$  and  $E'$  are the energies of the incoming and scattered electrons respectively. This range in  $y$  corresponds to a range of the energy of the  $\gamma p$  system ( $W$ )

of  $150$  GeV to  $250$  GeV. The cut removes events from the tails of the electron energy distribution where the acceptance is small. The photon virtuality  $Q^2$ , given by

$$Q^2 = 4EE' \cos^2(\theta/2),$$

is restricted to values  $< 0.01$  GeV<sup>2</sup>. This range of  $Q^2$  is limited by the ranges of the detected energy and angle of the scattered electron in the electron detector. Results presented in this paper are for  $ep$  cross sections integrated over the kinematic range in  $y$  and  $Q^2$  given above.

A jet finding algorithm was applied to the events passing the above selection criteria. The definition of a jet is based on the transverse energy in the calorimeter contained within a cone of radius  $R = \sqrt{\Delta\eta^2 + \Delta\phi^2} = 1.0$ , where  $\Delta\eta$  and  $\Delta\phi$  (in radians) are pseudorapidity and azimuth intervals. Throughout this paper the transverse energy is defined with respect to the beam axis. Only calorimeter cells in the pseudorapidity range  $-2 < \eta_{\text{cell}} < 2.5$  were considered in the jet search. Within this region, we select the cone with the highest transverse energy in the event. The transverse energy  $E_t$  within the cone is calculated as the scalar sum of transverse energy of its component calorimeter cells. The cone axis is taken to be the vector pointing from the event vertex to the transverse energy centroid of all cells within the cone [10]. Cones with  $E_t > 7$  GeV are accepted as jets and the cells inside such cones are removed for the subsequent search of the next highest  $E_t$  cone in the event. The jet search in the event is stopped when no further jet cone with  $E_t > 7$  GeV can be found. For the analysis we used only jets with the axis inside the central pseudorapidity interval  $-1 < \eta < 1.5$ . A total of 256 events with 276 jets satisfying these criteria were selected for further analysis.

A potential source of background in this data sample is the accidental coincidence of a proton beam gas interaction with an electron scattered at small angle in the same event. This background contribution was estimated using data taken with a non-colliding proton bunch and the rate of the small angle electron detector alone. The expected contribution of 3 events was neglected in the following study.

The Monte Carlo (MC) simulations which were used for acceptance calculations and comparisons with the data, are based on the event generator

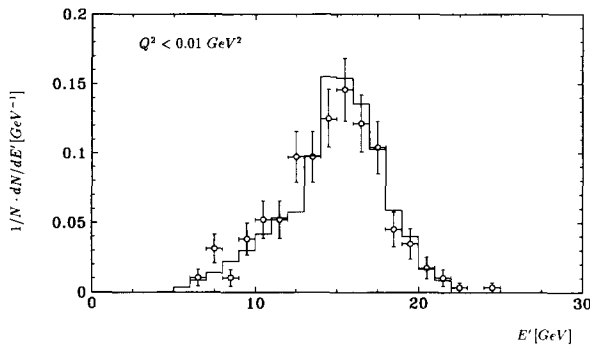


Fig. 1. Energy spectrum of the scattered electrons as measured by the small angle electron detector ( $\circ$ ) and predicted by simulation (histogram).

PYTHIA 5.6 [11]. The simulation of the  $ep$  collisions includes leading order QCD calculations for the hard scattering processes, summing the contributions from direct and resolved photon interactions. The effects of initial and final state QCD radiation are described by leading logarithm parton showers. Multiple parton interactions are not included. The hadronic fragmentation of the partons follows the Lund string model [12] as implemented in JETSET [11]. The generated events were fed into the H1 detector simulation program and subjected to the same reconstruction and analysis chain as the real data. The QED radiative corrections to the jet cross section are expected to be small ( $\lesssim 2\%$ ) for the present experimental conditions and are not considered in this analysis.

From MC simulation the mean overall efficiency of the trigger conditions and the selection criteria, including the geometrical acceptance of the electron detector, was determined to be  $(48 \pm 3)\%$ . This efficiency as a function of the energy of the scattered electron  $E'$  was used to calculate the cross sections given below. A comparison of the expected distribution of  $E'$  with that measured using the electron detector is in fig. 1 and it shows good agreement between data and MC.

The properties of the events containing high  $E_t$  jets were examined in terms of the transverse energy flow in the region around the jet axis. This is shown in fig. 2 in two ranges of  $\eta$  for jets with  $E_t > 7$  GeV as a function of  $\Delta\eta$  integrated over  $|\Delta\phi| < 1.0$  (fig. 2a, 2c) and as a function of  $\Delta\phi$  integrated over  $|\Delta\eta| < 1.0$  (fig. 2b, 2d). Here  $\Delta\eta$  and  $\Delta\phi$  are the coordinates of

a calorimeter cell in  $\eta$  and  $\phi$  relative to the jet axis.

The MC describes the jet profile well in the range  $-1.0 < \eta < 0.5$  (fig. 2a, 2b). However in the range  $0.5 < \eta < 1.5$  (fig. 2c, 2d) the data show larger average values of  $E_t$  outside the jet cone on the forward side of the jet than predicted by the MC. The contribution of this excess to the total  $E_t$  inside a jet cone is found to be almost independent of  $E_t$  and to increase with  $\eta$  of the jet. For jets with  $\eta = 1.5$  it is about 0.4 GeV and for jets in the barrel region with  $\eta < 1.0$  it is negligible. The difference in energy flow in the region close to the proton beam direction could possibly be attributed to an incorrect description of initial state radiation and spectator fragmentation effects in the simulation. We note that this difference may also be understood in the framework of models with multiple parton interactions. The uncertainty due to detector effects is taken into account in the analysis of systematic errors described below.

To obtain an inclusive jet cross section we corrected the observed jet rates for detector effects. Correction functions  $\epsilon(E_t)$  and  $\epsilon(\eta)$  were derived by comparing the transverse energy and pseudorapidity distributions for jets in reconstructed Monte Carlo events with those of generator jets. Generator jets were taken to be the jets found from the original final state particles using the same jet algorithm as for reconstructed events. For the determination of the correction functions (not for the comparisons of models with the data given below), the MC was weighted to describe the shape of the observed  $E_t$  and  $\eta$  dependence of the jet rates. No additional corrections were applied, either for the jet energy lost outside the jet cone, or for the non-jet energy contribution inside the cone. The obtained correction function  $\epsilon(E_t)$  by which the observed jet rates are to be multiplied was found to vary from about 1.3 to 1.0 over the range  $7 < E_t < 17$  GeV and  $\epsilon(\eta)$  from about 1.6 to 1.0 over the range  $-1.0 < \eta < 1.5$ . The  $E_t$  resolution determined by MC varied from about 2 GeV for jets with  $E_t = 7$  GeV to about 3 GeV for jets with  $E_t = 17$  GeV. The resolution in  $\eta$  was found to be about 0.2 in the whole  $\eta$  region.

The corrected  $ep$  inclusive jet cross section is given in fig. 3 and in table 1 as a function of  $E_t$  and pseudorapidity  $\eta$ . The cross sections rise strongly with  $\eta$  and decrease with transverse energy approximately as  $E_t^{-5.5}$ . The quoted errors receive contributions from statistics, systematic bin-to-bin uncertainties,

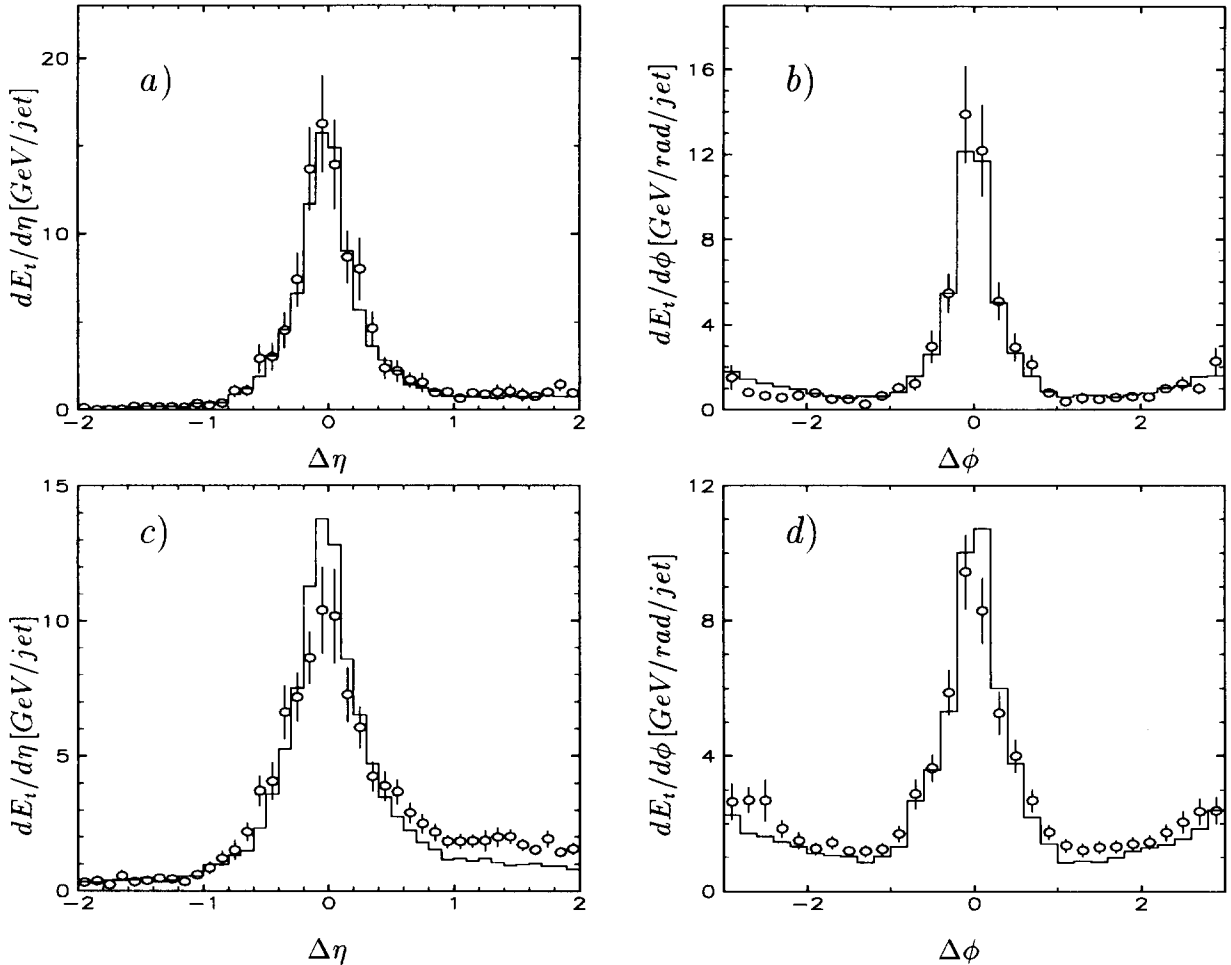


Fig. 2. Transverse energy flow in the region of the jet axis as a function of  $\Delta\eta$  integrated over  $|\Delta\phi| < 1.0$  (a), (c) and  $\Delta\phi$  integrated over  $|\Delta\eta| < 1.0$  (b), (d) for jets with  $E_t > 7$  GeV in the ranges  $-1.0 < \eta < 0.5$  (a), (b) and  $0.5 < \eta < 1.5$  (c), (d) for data ( $\circ$ ) and Monte Carlo (histogram).

and a scale error affecting only the overall cross section normalisation. Statistical and systematic bin-to-bin uncertainties are shown in table 1 and added in quadrature in fig. 3 (outer error bars). The inner error bars in fig. 3 represent the statistical errors only. The overall uncertainty of the cross section normalisation amounts to  $\pm 40\%$ .

In the following the contributions to the systematic uncertainties are described.

The hadronic energy scale of the LAr calorimeter based on beam tests [8] has been verified from the balance of transverse momentum between hadronic

jets and the scattered electron in deep inelastic events. The present estimate of the overall calorimeter energy scale uncertainty for hadronic jets amounts to an overall value of  $\pm 7\%$  allowing for an additional bin-to-bin contribution of  $\pm 4\%$  caused by possible systematic differences between calorimeter sections. These numbers are expected to improve in the future using high statistics data samples. Taking into account the steep slope of the inclusive jet cross section ( $E_t^{-5.5}$ ) the quoted energy scale uncertainties correspond respectively to  $\pm 38\%$  and  $\pm 22\%$  uncertainty in the cross section. For these present low energy measurements,

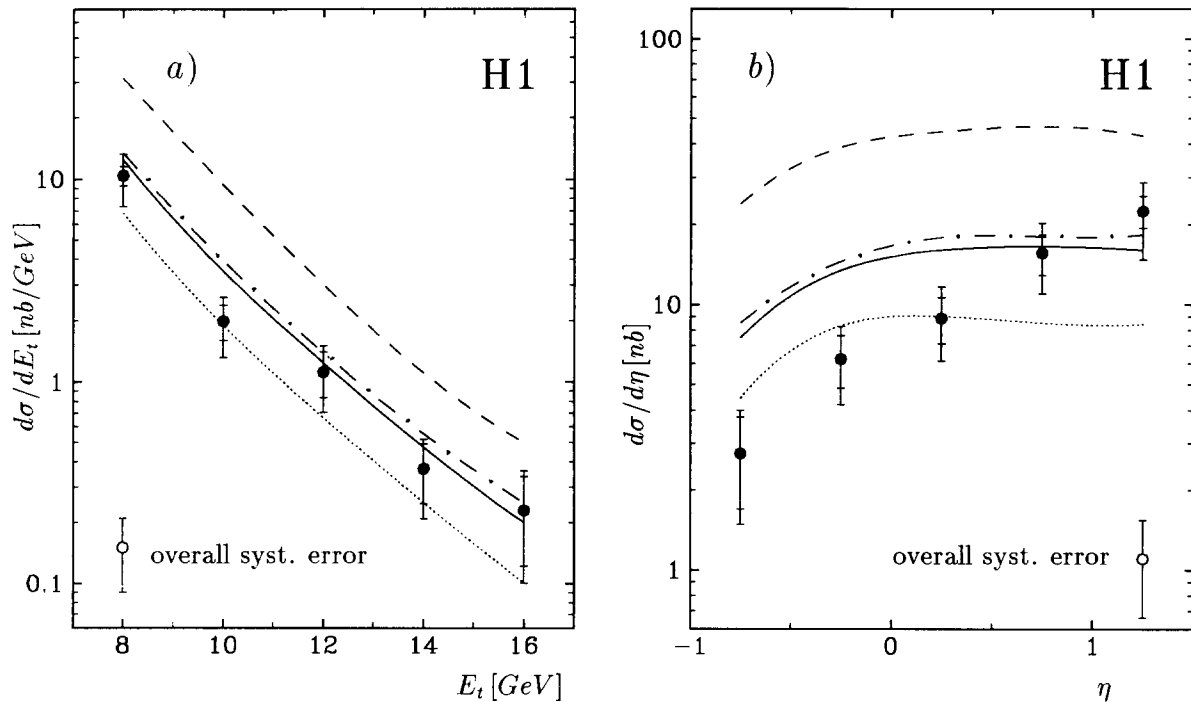


Fig. 3. Inclusive jet  $E_t$  spectrum (a) integrated over the pseudorapidity interval  $-1.0 < \eta < 1.5$  and inclusive  $\eta$  spectrum (b) for jets with  $E_t > 7$  GeV. The inner error bars represent the statistical errors, the outer error bars the statistical and bin-to-bin systematic errors added in quadrature. The overall systematic uncertainty of  $\pm 40\%$  is indicated. The curves show leading-order QCD calculations in the framework of the PYTHIA event generator using the photon structure functions LAC-3 (dashed line), LAC-2 (dashed-dotted line), GRV-LO (full line) and GRV-LO, but excluding the gluons originating from the photon (dotted line).

the uncertainty in the jet energy resolution contributes 10% to the overall systematic error. The determination of the correction functions  $\epsilon(E_t)$  and  $\epsilon(\eta)$  give rise to bin-to-bin uncertainties of  $\pm 10\%$ . The latter

were determined by varying the the shape of the MC spectrum within the range of errors of the measured spectrum. Trigger efficiency and luminosity measurement have uncertainties of  $\pm 6\%$  and  $\pm 7\%$  respectively, which go into the overall normalisation error. We make the conservative assumption that the lack of transverse energy close to the proton beam direction for the Monte Carlo relative to the data (discussed above and shown in fig. 2) may be attributed entirely to deficiencies in the detector description, which gives rise to a 20% additional systematic error for forward jets ( $\eta > 1$ ). The different contributions to the uncorrelated part of the systematic error are added quadratically and given in table 1.

Table 1  
Inclusive jet  $ep$  cross section for  $E_t > 7$  GeV and  $-1.0 < \eta < 1.5$  averaged over the range  $0.25 < y < 0.7$  and  $Q^2 < 0.01$  GeV<sup>2</sup>. Statistical and systematic bin-to-bin errors are given. Not included is an overall systematic error of  $\pm 40\%$ .

$E_t$ (GeV)	$d\sigma/dE_t$ (nb/GeV)	$\eta$	$d\sigma/d\eta$ (nb)
7-9	$10.4 \pm 1.1^{+2.6}_{-2.8}$	-1.0-0.5	$2.7 \pm 1.0 \pm 0.7$
9-11	$2.0 \pm 0.4^{+0.5}_{-0.5}$	-0.5-0.0	$6.2 \pm 1.4 \pm 1.5$
11-13	$1.1 \pm 0.3^{+0.3}_{-0.3}$	0.0-0.5	$8.8 \pm 1.7 \pm 2.1$
13-15	$0.37 \pm 0.12^{+0.09}_{-0.10}$	0.5-1.0	$15.6 \pm 2.7 \pm 3.8$
15-17	$0.23 \pm 0.11^{+0.06}_{-0.06}$	1.0-1.5	$22.4 \pm 3.1^{+5.4}_{-7.1}$

We compare the data in fig. 3 with predictions for the jet cross section based on the event generator PYTHIA discussed above. It should be noted that the predictions for jets with  $E_t > 7$  GeV are independent of the minimum momentum transfer,  $P_{t,min}$ , in the

hard scattering process, providing  $P_{t,\min}$  is less than 3 GeV. Uncertainties in the proton structure function have little influence on the predictions. Most of the Bjorken  $x$  range of the proton structure function relevant for the present jet sample ( $x > 0.01$  in about 85% of the events and  $\langle x \rangle \approx 0.08$ ) is covered by recent experiments [13]. We use a recent leading order parametrization GRV [14] of the proton structure function. The predictions for the jet rates differ by less than 10% using other recent leading order parametrizations [15].

We study the sensitivity to the photon structure function by using three leading order QCD parametrizations which differ mainly in the gluon densities. The MC prediction using the parametrization of Glück et al. [16] (GRV-LO) is shown together with predictions using two parametrizations of Abramowicz et al. [17], the sets 2 and 3 (LAC-2 and LAC-3), the latter of which assumes a very high gluon density at large  $x_\gamma$ . Here  $x_\gamma$  refers to the momentum fraction which the parton from the photon carries into the hard process. To demonstrate the sensitivity to the gluon content of the photon, we also show the predicted cross section due to parton sub-processes initiated only by quarks, and not by gluons, in the photon (dotted line) using the GRV-LO parametrization of the photon structure function. The measured jet cross section is consistent with that expected due to hard processes initiated by quarks in the photon allowing for a substantial contribution from gluon initiated processes.

The shape of the inclusive jet cross section  $d\sigma/dE_t$  is well described by the predictions in the covered range  $-1.0 < \eta < 1.5$ . The cross section calculated with LAC-3, however, is higher than the data by a factor of 3, while GRV-LO and LAC-2 are compatible with the data. The cross section  $d\sigma/d\eta$  shows a steeper rise with  $\eta$  than predicted by the models.

Recent next to leading order QCD calculations for jet photoproduction show that the corrections to the leading order jet cross section amount to  $\lesssim 20\%$  for a cone size  $R \approx 1$  [18,19].

We have presented the first measurement of inclusive jet cross sections for the interaction of electrons scattered at small angles ( $Q^2 \leq 0.01 \text{ GeV}^2$ ) with protons. The cross sections correspond to center of mass energies of the virtual photon-proton system between 150 and 250 GeV ( $0.25 < y < 0.7$ ). Within the

central interval of pseudorapidity  $-1 < \eta < 1.5$  the jet cross section decreases with transverse energy like  $E_t^{-5.5}$ . This shape is well described by leading order QCD calculations using the PYTHIA event generator. None of the models, however, describe well the measured  $\eta$  dependence.

We are very grateful to the HERA machine group whose outstanding efforts made this experiment possible. We acknowledge the support of the DESY technical staff. We appreciate the big effort of the engineers and technicians who constructed and maintained the detector. We thank the funding agencies for financial support of this experiment. The non-DESY members of the collaboration also want to thank the DESY directorate for the hospitality extended to them. Finally we would like to thank G. Kramer and S. G. Salesch for useful discussions.

## References

- [1] H1 Collab., T. Ahmed et al., Phys. Lett. B 297 (1992) 205.
- [2] ZEUS Collab., M. Derrick et al., Phys. Lett. B 297 (1992) 404.
- [3] W. Stirling and Z. Kunszt, Proc. HERA Workshop, DESY, Hamburg (1987), ed. R.D. Peccei, Vol. 1, p. 331.
- [4] AMY Collab., R. Tanaka et al., Phys. Lett. B 277 (1992) 215.
- [5] F. Brasse, The H1 Detector at HERA, to be published in the Proc. of the 26th Intern. Conf. on High Energy Physics, Dallas, 1992 and DESY preprint 92-140 (1992);  
G. Cozzika, The H1 Detector, to be published in the Proc. of the 3rd Intern. Conf. on Calorimetry in High Energy Physics, Corpus Christi, 1992, and DAPNIA preprint SPP-92-29 (1992).
- [6] H1 Collab., The H1 detector at HERA, to be submitted to Nucl. Instrum. Methods.
- [7] H1 Calorimeter Group, B. Andrieu et al., The H1 Liquid Argon Calorimeter System, DESY preprint 93-078 (1993), submitted to Nucl. Instrum. Methods.
- [8] H1 Calorimeter Group, B. Andrieu et al., DESY preprint 93-047 (1993), to be published in Nucl. Instrum. Methods.
- [9] H1 Collab., T. Ahmed et al., Phys. Lett. B 299 (1993) 374.
- [10] J.E. Huth et al., Toward a standardization of jet definitions, Fermilab-Conf-90/249-E (1990).

- [11] T. Sjöstrand, CERN-TH-6488 (1992);  
H.-U. Bengtsson and T. Sjöstrand, *Comput. Phys. Commun.* 46 (1987) 43;  
T. Sjöstrand and M. Bengtsson, *Comput. Phys. Commun.* 43 (1987) 367.
- [12] B. Andersson, G. Gustafson and T. Sjöstrand, *Phys. Lett. B* 94 (1980) 211;  
B. Andersson, G. Gustafson, G. Ingelman and T. Sjöstrand, *Phys. Rep.* 97 (1983) 31.
- [13] BCDMS Collab., A.C. Benvenuti et al., *Phys. Lett. B* 223 (1989) 485;  
NMC Collab., P. Amaudruz et al., *Phys. Lett. B* 295 (1992) 159.
- [14] M. Glück, E. Reya and A. Vogt, *Z. Phys. C* 53 (1992) 127.
- [15] J.G. Morfin, W.K. Tung, *Z. Phys. C* 52 (1991) 13;  
J.F. Owens, *Phys. Lett. B* 266 (1991) 126.
- [16] M. Glück, E. Reya and A. Vogt, *Phys. Rev. D* 46 (1992) 1973.
- [17] H. Abramowicz, K. Charchula and A. Levy, *Phys. Lett. B* 269 (1991) 458.
- [18] L.E. Gordon and J.K. Storrow, *Phys. Lett. B* 291 (1992) 320.
- [19] G. Kramer and S.G. Salesch, DESY preprint 93-010 (1993).